Journal of Power Sources 195 (2010) 4350–4355

Contents lists available at ScienceDirect

Journal of Power Sources

journal homepage: www.elsevier.com/locate/jpowsour

Silver nanoparticle-decorated carbon nanotubes as bifunctional gas-diffusion electrodes for zinc–air batteries

T. Wang, M. Kaempgen*, P. Nopphawan, G. Wee, S. Mhaisalkar, M. Srinivasan**

School of Materials Science and Engineering, Nanyang Technological University, Block N4.1, 50 Nanyang Avenue, Singapore 639798, Singapore

ARTICLE INFO

Article history:
Received 14 September 2009
Received in revised form
25 November 2009
Accepted 8 December 2009
Available online 18 January 2010

Keywords:
Carbon nanotubes
Silver decoration
Gas-diffusion electrode
Zn–air battery

ABSTRACT

Thin, lightweight, and flexible gas-diffusion electrodes (GDEs) based on freestanding entangled networks of single-walled carbon nanotubes (SWNTs) decorated with Ag nanoparticles (AgNPs) are tested as the air-breathing cathode in a zinc–air battery. The SWNT networks provide a highly porous surface for active oxygen absorption and diffusion. The high conductivity of SWNTs coupled with the catalytic activity of AgNPs for oxygen reduction leads to an improvement in the performance of the zinc–air cell. By modulating the pH value and the reaction time, different sizes of AgNPs are decorated uniformly on the SWNTs, as revealed by transmission electron microscopy and powder X-ray diffraction. AgNPs with sizes of 3–5 nm double the capacity and specific energy of a zinc–air battery as compared with bare SWNTs. The simplified, lightweight architecture shows significant advantages over conventional carbon-based GDEs in terms of weight, thickness and conductivity, and hence may be useful for mobile and portable applications.

1. Introduction

Zinc–air batteries, both primary [1–3] and rechargeable [4,5], are promising energy storage devices due to their high specific energy (100 Wh kg^{-1}), low cost and environmental friendliness. They are presently used in hearing aids and military applications and are considered an attractive alternative for powering electric vehicles and portable electronic devices when compared with high-cost Li-ion cells which have safety issues [6]. Zinc–air batteries obtain their specific energy advantage over other batteries since only one active component, the zinc metal anode, is stored in the battery; the reactant (oxygen) for the cathode is drawn from the air utilizing a gas-diffusion electrode (GDE) or air cathode. During cell operation (discharge), oxygen adsorbed from the surrounding air is reduced ($O_2 + 2H_2O + 4e^- \rightarrow 4OH^-$) using an oxygen reduction catalyst at the cathode, while the zinc metal (anode) is oxidized ($Zn + 4OH^- \rightarrow 2ZnO + 2H_2O + 4e^-$), and this leads to a usable electric current flow through an external circuit.

Gas-diffusion electrodes, which are vital for good zinc–air battery performance, are usually composed of carbonaceous powder pressed on to both sides of a metallic nickel mesh current-collector (Fig. 1), along with a binder for mechanical stability of the carbon layers, a hydrophobic additive (e.g., polytetrafluoroethylene, PTFE) on the air-facing side to avoid flooding of the pores with electrolyte, and a catalyst layer to promote oxygen reduction. Such a GDE multilayer electrode architecture is complex and is several hundred microns thick. Its weight is dominated by the metallic mesh current-collector that holds the carbon layers together [1].

Single-walled carbon nanotube (SWNT) networks can potentially replace the complex multilayer carbon-based GDE architecture because SWNTs form very thin and freestanding entangled networks (so called 'bucky papers') which are not only highly conducting and porous but also mechanically robust in terms of abrasion and bending. Hence, neither current-collectors nor binders are required, and SWNT networks can be used as the sole material for GDEs, to give a simplified single-layer electrode architecture that reduces weight, thickness, and manufacturing costs (Fig. 1). Studies have demonstrated the bifunctionality of such an architecture for supercapacitors [7], Zn/MnO_2 batteries [8], and fuel cells [9,10]. Previous investigations on carbon nanotubes for GDEs [11,12] still employed a conventional multilayer GDE architecture with binders and nickel mesh current-collectors.

Silver nanoparticles (AgNPs) function as catalysts to enhance oxygen reduction at the GDE because they are excellent electrocatalysts for O_2 reduction in dilute alkaline solutions [13] and in highly concentrated alkaline solutions, wherein the electrocatalytic performance of silver (Ag) is reported to be superior to platinum [14]. In the present work, a novel cathode material, composed of SWNTs decorated with AgNPs (AgNP-SWNTs), is evaluated for use as a lightweight GDE in a zinc–air battery. The large surface area provided by the SWNTs, in combination with their high con-

* Corresponding author.
** Corresponding author. Tel.: +65 6790 4606; fax: +65 6790 9081.
E-mail address: madhavi@ntu.edu.sg (M. Srinivasan).

0378-7753/$ – see front matter © 2010 Elsevier B.V. All rights reserved.
doi:10.1016/j.jpowsour.2009.12.137

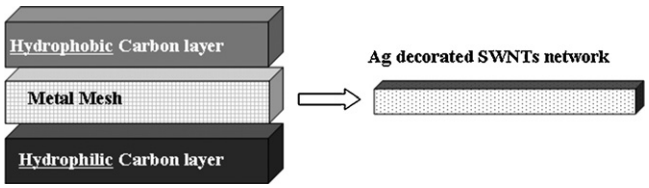

Fig. 1. Schematic of novel GDE architecture based on SWNTs (right) compared with commercial GDE using pressed carbon on nickel mesh (left).

ductivity, makes such networks an excellent support for catalyst particles. The application of this novel GDE architecture based on a single-layer AgNP-SWNT cathode is demonstrated, and the effect of AgNP particle size on the performance of a zinc–air battery is examined.

2. Experimental

2.1. AgNP decoration of SWNTs

An SWNT suspension was prepared using 0.8 g of functionalized SWNTs (P3, Carbon Solutions, Inc., Riverside, CA) in 15 ml of deionized water, followed by 20 min ultrasonication (120 kW). The SWNT suspension was then mixed with 0.15 M $AgNO_3$ solution (99.99 wt%, Aldrich, St. Louis, MO), and various amounts of 0.1 M NaOH (99 wt%, Merck, Whitehouse Station, NJ) were added to adjust the pH in a range from 4.3 to 7.3. Mixtures at different pHs were stirred for different times (15–120 min) in order to control the size of the AgNPs. The decorated SWNTs were separated from the solution by centrifugation (15,000 rpm, 10 min), and excess Na^+, Ag^+ and NO_3^- were removed by multiple washing steps with deionized water. The final product was then re-dispersed in deionized water.

2.2. Electrode fabrication

A suspension containing AgNP-decorated SWNTs (AgNP-SWNTs) with a concentration of 0.2 mg ml^{-1} in deionized water was filtered through a membrane (Whatman, 20 nm pore size, 47 mm diameter). The SWNTs (bare or Ag-decorated) were trapped on the surface of the filter to form an entangled interconnected network. After drying, the SWNT network was peeled from the filter film and used as a freestanding GDE without further treatment.

2.3. Characterization

AgNP-SWNTs were characterized by transmission electron microscopy (TEM, JEOL 2100F) in a high resolution mode operating at 200 kV, and by X-ray diffraction (XRD) using a Shimadzu diffractometer (Cu Kα) with step scanning (0.02°, 0.6 s dwell time) over a 2θ range of 10° to 140°. A four-point probe configuration was used to measure the resistivity and conductivity.

2.4. Electrochemical testing

Potentiodynamic polarization of the GDEs was performed by means of a potentiostat (GillAC, ACM instruments, Grange-Over-Sands, UK) in a three-electrode set-up. An Ag|AgCl electrode with a double junction and a platinum sheet were used as the reference electrode and counter electrode, respectively, and 6 M KOH (99.9 wt%, Aldrich) was used as the electrolyte. The scan rate was 1 mV s^{-1} for the potentiodynamic polarization and 20 mV s^{-1} over a potential range of −0.5 to +0.5 V for cyclic voltammetry.

2.5. Device fabrication and testing

The zinc anode was prepared by mixing zinc powder with polyvinylidene fluoride binder using 1-methyl-2-pyrrolidone (NMP) as solvent (weight ratio of Zn:PVDF:NMP = 4:1:9). The paste was heated to 85 °C for 4 h and then pressed into a pellet with a thickness of around 35 μm. The zinc–air battery was assembled by stacking the Zn-anode and AgNP-SWNTs air cathode separated by a Celgard 2400 polypropylene (PP, Celgard, LLC, Charlotte, NC) film wetted thoroughly with 6 M KOH electrolyte. The performance of various devices having SWNT-GDEs with AgNPs of different sizes was evaluated by discharging through a constant resistance of 1 kΩ. The voltage was monitored using a potentiostat (AFBP1, Pine Instrument Co., Grove City, PA). For comparison, commercially available GDEs (conventional GDEs) based on pressed carbon and catalyst on a nickel mesh (E4A Air Cathode, Electric Fuel Limited, Israel; ELAT® GDE product line, BASF, Germany) were also tested.

3. Results and discussion

3.1. Deposition of AgNPs on SWNTs

Deposition of AgNPs on SWNTs was carried out using $AgNO_3$ as the metal salt precursor and NaOH as the reductant. Transmission electron microscopic (TEM) images of AgNP-SWNTs (Fig. 2a–d) reveal a uniform AgNP distribution on the SWNTs. The AgNP size is dependent on pH and ageing time at a constant $AgNO_3$ concentration (0.15 M). Initially, the pH of the SWNT suspension drops from 5.6 to 3.4 on addition of $AgNO_3$ to the SWNT dispersion. This change in pH is due to the interaction of Ag^+ ions with the carboxyl functional groups (–COOH) of SWNTs to form $–COO^-Ag^+$ groups [15] and the subsequent release of H^+ ions. Addition of NaOH, which provides hydroxyl ions (OH^-), results in the reduction of Ag^+ ions which leads to Ag^0 precipitation according to the reaction $4\ –COO^-Ag^+ + 4OH^- \rightarrow 4\ –COO^- + 4Ag^0 + 2H_2O + O_2\uparrow$. A higher concentration of OH^- at pH 6.3 results in the precipitation of smaller AgNPs (6–8 nm; Fig. 2b), whereas pH 4.3 yields an AgNP size of 12–15 nm (Fig. 2a). Decreasing the reaction time from 120 to 60 min at pH 6.3 causes a further reduction in AgNP size to 3–5 nm (Fig. 2d). The decrease in AgNP size at higher pH may be due to a reaction between excess OH^- ions and Ag^+ ions in the suspension ($2Ag^+ + 2OH^- \leftrightarrow Ag_2O + H_2O$), thus decreasing the concentration of Ag^+ ions available for deposition and thereby lowering the growth rate of nucleated Ag metals. At lower pH values, more Ag^+ ions are available, potentially leading to a faster growth rate and larger particles.

The presence of AgNPs on the SWNTs was further confirmed by XRD (Fig. 2c). Diffraction peaks at 2θ = 38°, 45°, 64°, 78°, and 82°, in addition to the SWNT peak at 26°, show the formation of cubic Ag^0 nanoparticles (cubic space group $Fm\bar{3}m$ or 225). These reflections are in excellent agreement with previously published data on Ag-decorated multi-walled carbon nanotubes (MWNTs) [16].

3.2. Gas-diffusion electrode (AgNP-SWNT) characterization

The weight, thickness and conductivities of bare SWNT networks and AgNP-SWNT networks were compared with those of a conventional GDE based on pressed carbon on a nickel mesh, see Fig. 3. The weight and thickness of the SWNT samples are 0.005 mg cm^{-2} and 0.05 mm, respectively, as compared with 0.79 mg cm^{-3} and 0.49 mm for the conventional carbon-based electrode. Apparently, weight and thickness are reduced by more than one order of magnitude for the SWNT electrodes because of their single-layered architecture. Thus these electrodes would be of particular interest for portable devices where weight and space are

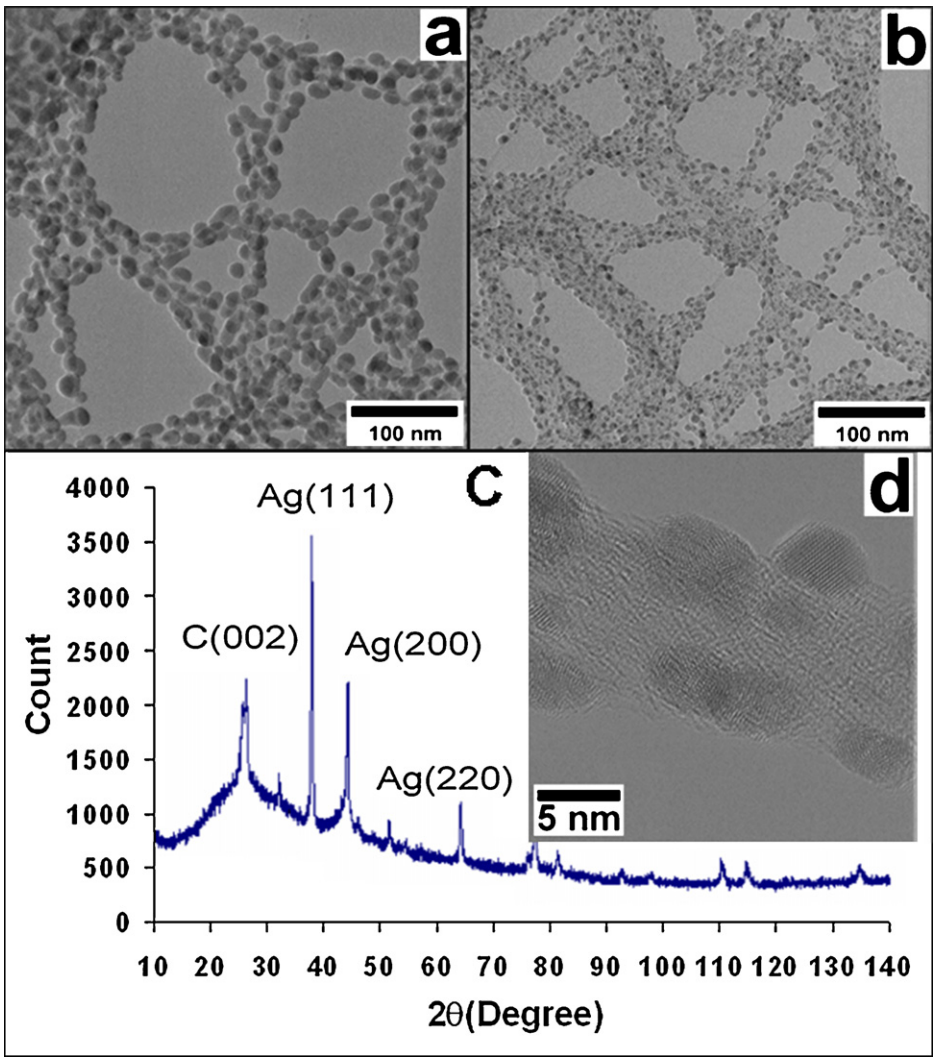

Fig. 2. Transmission electron microscopic images of SWNTs decorated with AgNP of various sizes (a) 12–5 nm, (b) 6–8 nm, and (d) 3–5 nm, and (c) representative powder XRD pattern of AgNP-SWNTs showing characteristics peaks of Ag.

crucial factors. The conductivity of the SWNT electrodes increases by around three orders of magnitude as compared with the conventional carbon-based GDEs, owing to the high conductivity of SWNTs. Among the GDEs based on SWNTs, the conductivity is significantly higher for the AgNP-decorated material (bare SWNT films: ~1000 S cm^{-1}; decorated SWNT films: 2000–3000 S cm^{-1}). The highest conductivity (~3000 S cm^{-1}) is obtained with the smallest Ag-particle size (3–5 nm), which can be explained by additional and less resistive current paths within the SWNT network provided by AgNP.

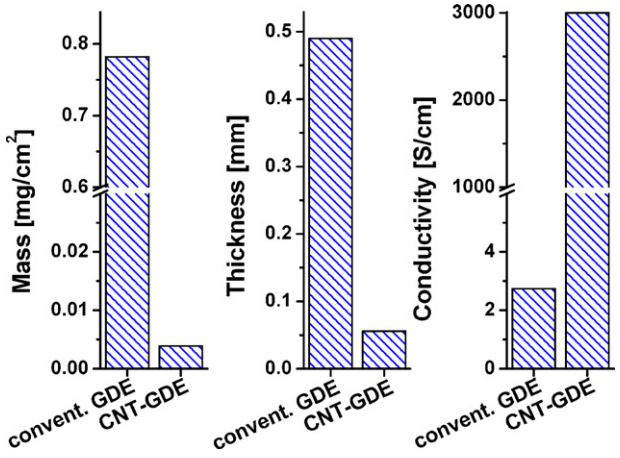

Fig. 3. Comparison of SWNT-based GDEs with commercial GDEs in terms of thickness, weight and conductivity.

The electrochemical behaviours of the AgNP-SWNT GDEs were investigated using cathodic potentiodynamic polarization and cyclic voltammetry with one side exposed to air and the other in contact with KOH electrolyte. The results were compared with a bare SWNT film and a conventional GDE electrode. The results for potentiodynamic polarization curves are shown in Fig. 4. The current is normalized by weight to account for any sample-to-sample variance while the area of all GDEs is kept constant (~1 cm^2). In general, the current densities of the AgNP-SWNTs are significantly higher than those of both bare SWNTs and the commercial air electrode. This is due to the high catalytic activity of Ag towards O_2 reduction on the AgNP-containing GDEs [3,17]. Also, it is observed that higher current densities are obtained for SWNT-GDEs containing smaller-sized AgNPs, which can be explained by the larger surface area. Upon examination of the relevant voltage for O_2 reduction at around 0.3 V (see also cyclic voltammograms in Fig. 5), it is apparent that the current density of the GDE containing the smallest Ag nanoparticles (3–5 nm) is larger by roughly a factor of

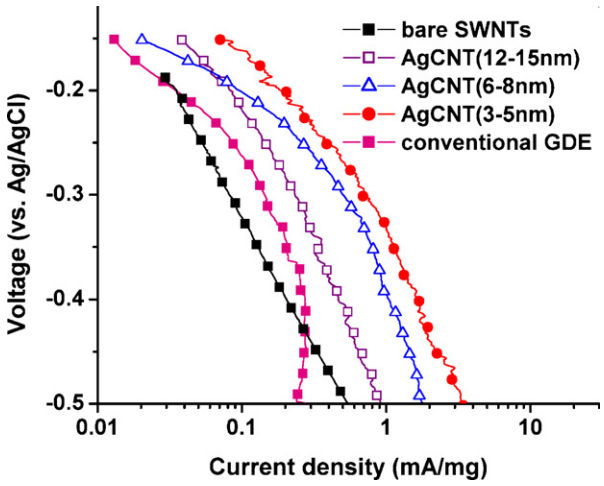

Fig. 4. Potentiodynamic polarization curves of bare SWNTs, commercial air electrode, and AgNP-SWNTs with different AgNP particle sizes.

10, than that of the bare SWNT electrode. In addition, the size of the silver particles is known to affect the mechanism of oxygen reduction that can proceed in alkaline electrolytes by two overall pathways, as follows:

$$\text{Directfour-electronpathway}: \quad O_2 + 2H_2O + 4e^- \rightarrow 4OH^- \qquad (1)$$

$$\text{Two-electron(orperoxide)pathway}: \quad O_2 + H_2O + 2e^- \rightarrow HO_2^- + OH^- \qquad (2)$$

Peroxide formed in the two-electron pathway undergoes subsequent reduction or decomposition to OH^- ions:

$$HO_2^- + H_2O + 2e^- \rightarrow 3OH^- \qquad (3)$$

$$2HO_2^- \rightarrow 2OH^- + O_2 \qquad (4)$$

The four-electron and the two-electron reduction occur at different active sites on the AgNP particles. For smaller AgNP particles, the two-electron pathway becomes dominant leading to higher current densities [18], which is consistent with our findings.

Cyclic voltammetry (CV) was employed to investigate the electrochemical redox behaviour of bare and AgNP-decorated SWNT GDEs (Fig. 5). For all samples, an O_2 reduction peak (R_{O_2}; $O_2 + 2H^+ + 2e^- \rightarrow H_2O_2$ [19]) was observed at −0.2 V vs. Ag|AgCl for GDEs containing AgNPs of 6–8 nm and 12–15 nm, and at −0.3 V vs. Ag|AgCl for AgNP of 3–5 nm and for the bare SWNT-GDE. The difference in potentials between decorated and bare SWNTs can be explained by a higher overpotential of the different materials towards O_2 reduction (for AgNP: $E = -0.2$ V; for SWNT: $E = -0.3$ V). The reduction potential of $E = -0.3$ V for the SWNT sample decorated with 3–5 nm AgNPs can be explained by a less pronounced coverage of the SWNTs by the AgNP, which allows the electrochemical properties of the SWNTs to dominate. For all AgNP-SWNT films, an additional oxidation and two reduction peaks are also observed. The oxidation peak appearing at around 0.3 V (labeled with 'O_{Ag}') is attributed to the oxidation of Ag to Ag_2O ($2Ag + 2OH^- \rightarrow Ag_2O + H_2O + 2e^-$). The first reduction peak at around 0.28 V (R_{Ag}) indicates the reduction of Ag_2O to Ag [20], while the second peak corresponds to the O_2 reduction discussed before. As for the bare SWNT sample, an additional peak is observed at around −0.1 V (Fig. 5, peak "C") and is due to the reaction of oxygen-containing functional groups [21]. Furthermore, it is also observed that the total current density ($mA\,cm^{-2}$) for all reduction processes increases when the Ag-particle size is decreased, which is in agreement with the cathodic polarization results described previously (Fig. 4). For a more detailed analysis, the total charge for O_2 reduction is analyzed by integrating the corresponding peaks of the CV, and the results are presented in Fig. 6. Hence, it is quantitatively observed that the charge for O_2 reduction increases significantly on Ag decoration of SWNTs, com-

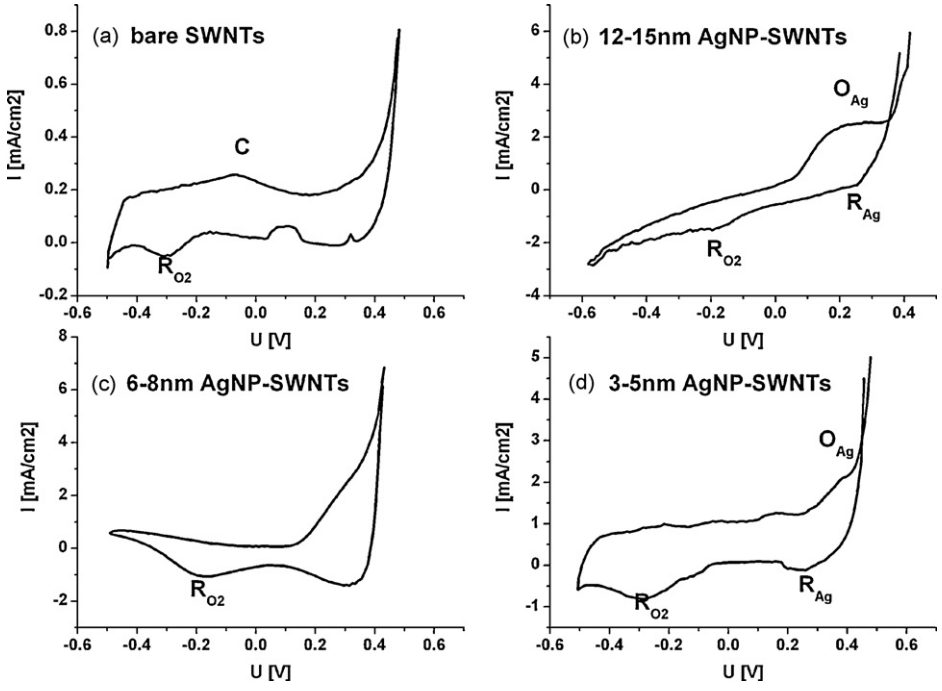

Fig. 5. Comparison of cyclic voltammograms (vs. Ag|AgCl) of AgNP-SWNTs with different particle sizes at scan rate of 10 mV s^{-1} in 6 M KOH (a–d).

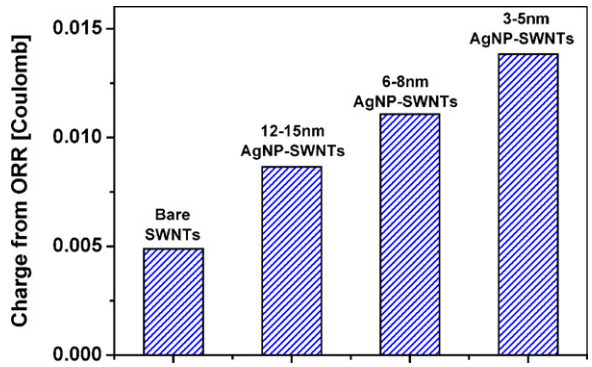

Fig. 6. Plot of charge from oxygen reduction reaction (ORR) of various GDEs obtained from their respective cyclic voltammograms (Fig. 5), showing dependence of total charge consumed for O_2 reduction on size of AgNPs.

pared with bare SWNTs. Decreasing AgNP size increases the total charge for the O_2 reduction reaction, which corroborates our earlier observation.

3.3. Device testing

For device testing, the AgNP-SWNT networks were used as GDE electrodes in a zinc–air battery configuration. Note that no binder, conductive additives, or water repellents such as PTFE were added to these proof-of-concept electrodes. The discharge characteristics using a 1 kΩ resistor are presented in Fig. 7. For all devices tested, the weight of Zn-containing anodes is constant, and therefore the observed differences in electrochemical behaviour can be attributed to differences between the AgNP-SWNT GDEs. The open-circuit voltages are around 1.2 V, which is in good agreement with the values for commercially available devices [22,23]. After connecting the device to a 1 kΩ load, the voltage drops according to the different conductivities of the GDEs.

Among the AgNP-SWNT GDEs, the smallest particle size seems to be favourable over the other particle sizes investigated. Not only is the voltage drop smaller due to the higher conductivity, but also the discharge curve is the flattest when compared with the other samples, indicating a less pronounced concentration polarization. In Table 1, the performances of all devices are summarized in terms of the conductivity of the SWNT film, specific capacity, C, and specific energy, E, using $C = I{\cdot}t{\cdot}{m_1}^{-1}$ and $E = I{\cdot}V{\cdot}t{\cdot}{m_2}^{-1}$, respectively, where I is the discharge current, t is the discharge time, V is the operating voltage, m_1 is the mass of the Zn-anode, and m_2 is the weight of the entire device including electrodes, separator and electrolyte. Compared with GDEs based on bare SWNTs, it is obvious that both C and E are improved by decoration of the SWNTs with Ag nanoparticles with diameters less than 8 nm. The best performance is achieved for GDEs with the smallest Ag nanoparticles (3–5 nm) investigated, with both the specific capacity and specific energy doubled. The improved performance with the smallest Ag-particle size can be explained by the fact that a larger electroactive surface leads to more catalytically active sites for O_2 reduction and, subsequently, to a higher current density.

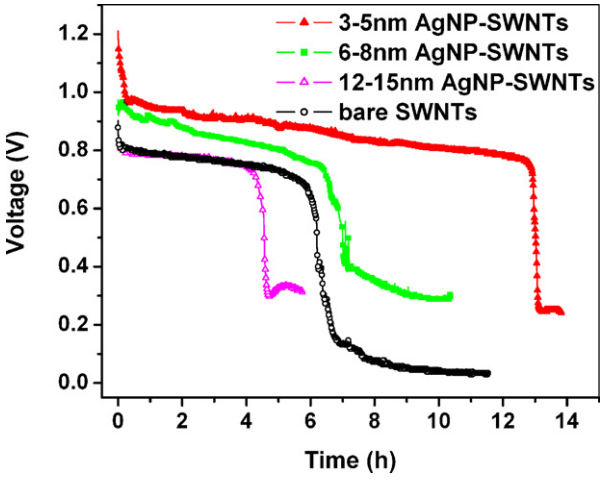

Fig. 7. Discharge with constant resistance of Zn–air batteries using GDEs based on AgNP-SWNTs with AgNPs of different sizes.

Table 1
Characteristics of zinc–air cells utilizing GDEs based on SWNT films decorated with Ag nanoparticles of different sizes.

Zn–air cells utilizing a GDE based on	Conductivity [S cm^{-1}]	Specific capacity[a] [mAh g^{-1}]	Specific energy density[a] [Wh kg^{-1}]
Bare SWNTs	1025	270	125
12–15 nm AgNP-SWNTs	1840	170	85
6–8 nm AgNP-SWNTs	3020	340	180
3–5 nm AgNP-SWNTs	3090	515	300
Conventional GDEs	2.74	200–600	250–400

[a] Specific capacity is normalized to the mass of the Zn-anode while specific energy is normalized to the mass of the entire device including electrodes, separator and electrolyte. For comparison, the performance range of commercially available GDEs [20–22] is listed.

In general, the performance of the GDEs based on AgNP-SWNTs is already comparable with commercial devices, where it is typical to observe capacities of 200–600 mAh g^{-1} and specific energies of 300–400 Wh kg^{-1} [22–24]. Hence, further optimization of the novel SWNT-based GDEs decorated with AgNPs is a promising approach to expand the application range of Zn–air batteries towards higher performance demands.

4. Conclusions

GDEs based on SWNT networks lead to a significant weight reduction when compared with carbon-based GDEs. In addition, decoration of SWNTs with Ag nanoparticles promotes O_2 reduction and thereby provides a significant improvement in terms of the specific capacity and specific energy of zinc–air battery. The optimum AgNP catalyst particle size is found to be the smallest (3–5 nm) among the samples investigated, resulting in a doubling of the specific capacity and specific energy when compared with bare SWNT-based GDEs. Hence, SWNTs decorated with Ag nanoparticles are promising materials for GDEs in lightweight applications with higher performance demands.

References

[1] W.H. Zhu, B.A. Poole, D.R. Cahela, B.J. Tatarchuk, J. Appl. Electrochem. 33 (2003) 29.
[2] F. Beck, P. Rüetschi, Electrochim. Acta 45 (2000) 2467.
[3] C.Y. Wu, P.W. Wu, P. Lin, Y.Y. Li, Y.M. Lin, J. Electrochem. Soc. 154 (2007) B1059.
[4] C. Chakkaravarthy, A.K. Abdul Waheed, H.V.K. Udupa, J. Power Sources 6 (1981) 203.
[5] AER Energy Resources Inc., Smyma, GA, USA; Revolt Technology, Zurich, Switzerland; Evionyx, Hawthorne, NY, USA.
[6] S. Megahed, B. Scrosati, J. Power Sources 51 (1994) 79.
[7] M. Kaempgen, J. Ma, G. Gruner, G. Wee, S.G. Mhaisalkar, Appl. Phys. Lett. 90 (2007) 264104.
[8] A. Kiebele, G. Gruner, Appl. Phys. Lett. 91 (2007) 144104.
[9] M. Kaempgen, M. Lebert, M. Soehn, N. Nicoloso, S. Roth, J. Power Sources 180 (2008) 755.
[10] M. Kaempgen, M. Lebert, N. Nicoloso, S. Roth, Appl. Phys. Lett. 92 (2008) 094103.
[11] H. Huang, W. Zhang, M. Li, Y. Gan, J. Chen, Y. Kuang, J. Colloid Interface Sci. 284 (2005) 593.
[12] G.-Q. Zhang, X.-G. Zhang, Y.-G. Wang, Carbon 42 (2004) 3097.

[13] B.B. Blizanac, P.N. Ross, N.M. Markovic, Electrochim. Acta 52 (2007) 2264.
[14] M.A. Kostowskyj, R.J. Gilliam, D.W. Kirk, S.J. Thorpe, Int. J. Hydrogen Energy 33 (2008) 5773.
[15] T.W. Ebbesen, H. Hiura, M.E. Bisher, M.M.J. Treacy, J.L. Shreeve-Keyer, R.C. Haushalter, Adv. Mater. 8 (1996) 155.
[16] A. Zamudio, A.L. Elias, J.A. Rodriguez-Manzo, F. Lopez-Urias, G. Rodriguez- Gattorno, F. Lupo, M. Ruhle, D.J. Smith, H. Terrones, D. Diaz, M. Terrones, Small 2 (2006) 346.
[17] S. Gamburzev, K. Petrov, A.J. Appleby, J. Appl. Electrochem. 32 (2002) 805–809.
[18] Y. Yang, Y. Zhou, J. Electroanal. Chem. 397 (1995) 271–278.
[19] J. Pichumani, K.S.V.S. Britto, J.A.A. Angel Rubio, P.M. Ajayan, Adv. Mater. 11 (1999) 154.
[20] F.H.B. Lima, C.D. Sanches, E.A. Ticianelli, J. Electrochem. Soc. 152 (2005) 1466.
[21] J.N. Barisci, G.G. Wallace, R.H. Baughman, J. Electroanal. Chem. 488 (2000) 92.
[22] D. Linden, in: B. Thomas, Reddy (Eds.), Handbook of Batteries, 3rd edition, McGraw-Hill, 2001.
[23] C.C. Chan, K.T. Chau, Modern Electric Vehicle Technology, Oxford University Press, 2001.
[24] Duracell®, Technical Bulletin on Zn–Air Cells, http://www.duracell.com.